# A multiwavelength digital holographic microscope architecture for enhancing life detection

**J. Kent Wallace**
**Eugene Serabyn**
**Chris Lindensmith**
**Jet Propulsion Laboratory/**
**California Institute of Technology**
**4800 Oak Grove Dr.**
**Pasadena, CA 91109**
**818-393-7066**
**James.K.Wallace@caltech.edu**
**Eugene.Serabyn@caltech.edu**
**Christian.Lindensmith@caltech.edu**

**Jay Nadeau**
**Department of Physics**
**Portland State University**
**Portland, OR 97201**
**503-795-8929**
**nadeau@pdx.edu**

**Stephanie Rider**
**Manuel Bedrossian**
**Division of Aerospace Engineering**
**California Institute of Technology**
**1200 E. California Blvd.**
**Pasadena, CA 91125**
**626-395-4057**
**srider@caltech.edu**
**mbedross@caltech.edu**

*Abstract*—**Spectral properties of living organism can provide a discriminating method for characterization. However, digital holographic microscopy (DHM), a high-resolution, volumetric imaging technique that is well-suited for examining microbial species is typically monochromatic. Thus, the spectral properties of bacteria are not probed with DHM save only for the wavelength of operation. Here we describe a new DHM instrument which enhances the method via the simultaneous recording of wavelength multiplexed holograms of the sample. This coarse spectral encoding is akin to labeling with RGB values, thereby producing colorized images of the species which enables a new dimension of characterization. This new instrument is derived from a previous architecture which has already demonstrated superior opto/mechanical stability. Herein, this novel instrument is described, and the results of experimental measurements taken with this new instrument are shown.**

## TABLE OF CONTENTS

1. INTRODUCTION.....1
2. INSTRUMENT DESCRIPTION.....1
3. EXPERIMENTAL DATA .....4
7. SUMMARY .....4
ACKNOWLEDGEMENTS.....4
REFERENCES .....5
BIOGRAPHY .....5

## 1. INTRODUCTION

Many living organisms can be characterized by their unique spectral response – both in emission and absorption. For instance – chlorophyll, green fluorescent protein (GFP), and certain halophilic bacteria such as chromohalobacter beijerinckii all have strong spectral features that originate at the cellular level. Therefore, when examining microscopic samples, measuring a spectral response can provide key identifying and discriminating information about the sample itself, but also the location of biological processes within the cell.

Holography is a method well suited to microbial studies [1-5]. It provides high spatial resolution (resolving features < 1.0 μm) and over a large sample volume (~ 0.5 μm x 0.5 mm x 1 mm). When holograms are captured at video rates, this volumetric information can be played back as a movie, thus providing insight into the 3D motility patterns of the species under study. However, our previous holographic instruments operated monochromatically, and thus gave amplitude and phase information about the sample at a single wavelength only.

Our monochromatic architecture has been demonstrated to largely remove instrumental error sources (such as vibration and alignment sensitivity) while also maintaining the intrinsic sensitivity and resolution of the method [6]. This instrument has been successfully fielded to harsh environs where its capabilities were severely tested. It passed with flying color – for that instrument was monochromatic, operating only a single wavelength. Recognizing the need for chromatic characterization, the instrument has been re-engineered to be polychromatic.

Below, we first describe the monochromatic instrument, then describe the architecture for the multi-wavelength instrument. We describe the additional processing required for the multiwavelength instrument, then illustrate its performance.

## 2. INSTRUMENT DESCRIPTION

### *A. Monochromatic, common-mode architecture*

The starting point for this instrument was our previous DHM instrument which we refer to as the 'common-mode' design. The instrument is shown schematically in Figure 1. It is described in greater detail elsewhere, so here we provide only a cursory overview.

A single-mode fiber source is first collimated with a collimator lens. The source light itself is provided by a 405-nanometer wavelength laser diode. This light, collimated by

978-1-5386-6854-2/19/$31.00 ©2019 IEEE

the lens, then illuminates two sample chambers: one is a reference sample of clear, empty, aqueous solution and the other is the science sample which is identical to the reference sample save for the addition of the object under study (nominally a microbial species of some type). These two sample chambers, reference and science, are made in the sample substrate, and thus share the same optical components. The difference being that the sample chambers are laterally offset from one another by a few millimeters. Two objective lenses (NA=0.37) immediately follow the sample chambers. The science beam is nominally collimated, while the reference beam – having passed through the sample chamber unaffected – forms a focus. In the back focal length of the science beam is the science pupil. In the back focal length of the reference beam is the reference focus. The subsequent relay lens performs two operations: 1) it forms an image of both the specimen and the reference chambers, and 2) it over lays them on the detector array thereby producing interference fringes. The lateral separation of the two objective lenses, and the focal length of the relay lens are paired such that the resulting fringes are properly sampled by the pixels on the imaging array. That sampling is such that: 1) an object PSF is sampled by ~ 3 pixels, and 2) that PSF is modulated by a full interference fringe.

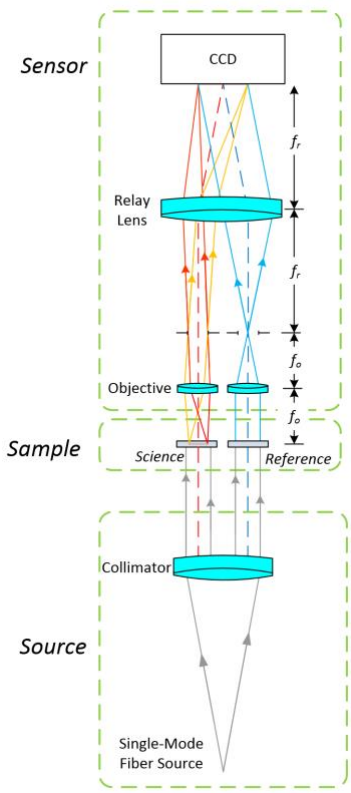


**Figure 1. Diagram of the common-mode digital holographic microscope**

In this configuration, the fringes are uniquely oriented along the imaging array – they are orthogonal to the vector that defines the center-to-center separation between the two objectives.

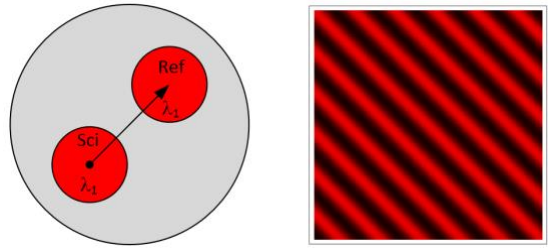


**Figure 2. The orientation of the objectives is shown on the left (both science and reference beams). On the right is shown the fringe orientation on the detector.**

This optical configuration results in a very robust instrument which is insensitive to mechanical vibrations, thermal changes, and optical misalignments. It has been successfully fielded to several different extreme environments and operated successfully.

During numerical processing [10], the raw interferogram measured on the array is 2D Fourier transformed. The resulting 2D Fourier Transform (when re-centered such that the zero spatial frequency occurs at the center of the array) can be characterized by a circular central portion that is the autocorrelation, and two, circular satellite regions that are symmetric about the center of the array. These satellites are the convolution of: 1) the 2D Fourier transform of the original object and 2) two delta functions at the spatial frequency of the fringe (the 2D Fourier transform of a cosine fringe). Selecting one of these satellite regions and inverse transforming will give the full, complex electric field of the sample at the nominal imaging plane (U(0)). The field can be numerically propagated to a new z distance via the following operation

$$U(z;\lambda) = 2DFFT[I2DFFT[U(0)\ G[z;\lambda]] \qquad (1)$$

Here, 2DFFT represents the 2D Fourier transform, and I2DFFT represents the inverse 2D Fourier transform. The diffraction kernel is represented by $G[z;\lambda]$ and is given by the following expression

$$G[z;\lambda] = Exp[-i\ (2\pi z/\lambda)\ Sqrt[1-(\lambda\xi)-(\lambda\eta)]] \qquad (2)$$

Where z is the propagation distance, $\lambda$ is the wavelength of operation, and $\xi$ and $\eta$ are the spatial frequency coordinates in the Fourier transform space. These numerical methods for off-axis DHM processing are well described in the literature [5]. We will return to this when we discuss the multi-wavelength implementation.

DHM enables the direct measurement of the electric field in object plane. Once this electric field is measured, it can be numerically propagated to any other plane of interest.

*B. Multi-wavelength, common-mode architecture*

Other multi-wavlength DHMs have been constructed and demonstrated. However, they tend to be somewhat bulky and

sensitive to alignment [7,8,9]. Here, our design follows from the lessons learned from our original instrument. The multi-wavelength implementation modifies the original system in the following ways: 1) the monochromatic source is replaced by a source with three unique wavelengths 2) the pair of objectives is replaced by objectives with a system of objects having a single, science objective at the center, surrounded by three, wavelength dependent objectives. The wavelength for a given reference beam is determined by an optical bandpass filter that is in-line with only one of the reference objectives. These bandpass filters had to be specified such that the substrate thickness was identical in order to maintain the optical path length between the science beam and each of the three reference beams. A clear, AR coated substrate of the same glass and optical thickness was placed in the science beam path as well.

The central, science objective is illuminated by all three wavelengths simultaneously. In the final focal plane, on the imaging array, three sets of fringes are formed, each with a unique orientation. Each set of fringes is normal to the vector that defines the center-to-satellite objective for that wavelength. Because there are three orientations of satellite objective lenses with respect to the center objective, there are three fringe orientations on the array. This is shown in Figure 2 below.

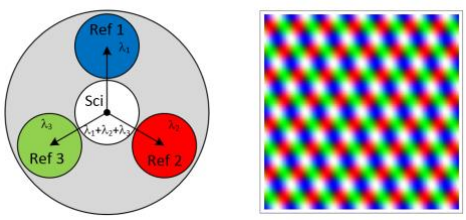


**Figure 2. The figure on the left shows the geometry of the color filters for the multi-wavelength, and the image on the right show the resulting fringe pattern.**

The sample chamber was modified as well. The nominal design of the sample chamber is a microfluidics chamber formed by sandwiching a watertight gasket between two pieces of optical glass. The central portion of sample chamber contained the bacterial sample. A single, large continuous chamber arched between the three reference beam paths and contained a reference solution that was uncontaminated. This is illustrated below in Figure 3.

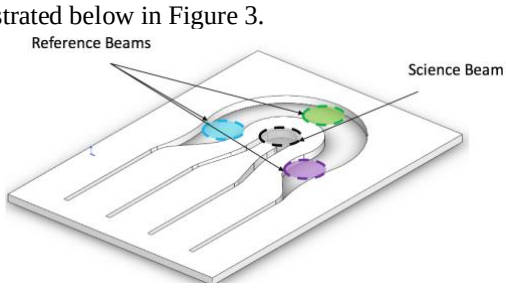


**Figure 3. The multiwavelength sample chamber has a central area for the science beam to pass, while the references beams pass around.**

The full architecture of the multi-wavelength system is shown below in Figure 4. In practice, a fiber combiner is used to mix the three independent wavelengths.

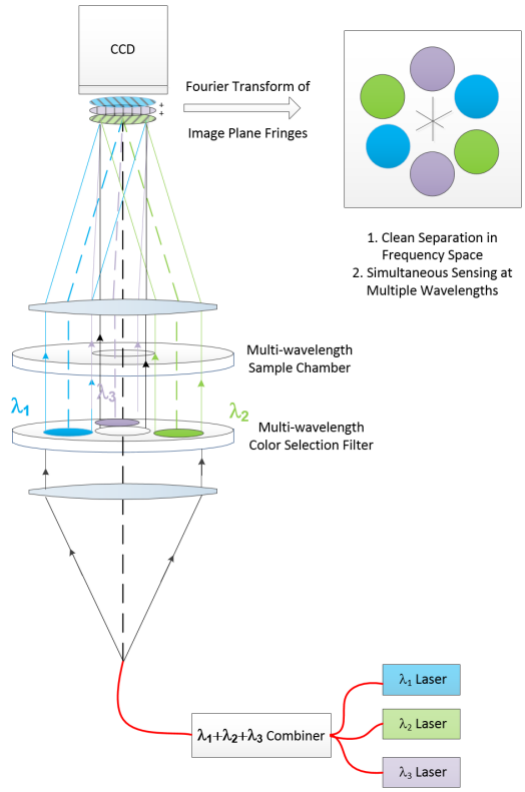


**Figure 4. The functional diagram of the multi-wavelength system is shown above. Here, wavelength combination is done via a fiber-combiner. In Fourier space, the different wavelengths are cleanly separated, thus turning a black and white camera into a color camera in post processing.**

The change in the light source, the objective lens assembly, and the sample chamber are the only changes to the hardware of the system. The other optics (collimator lens, the relay lens), and the detector were all unchanged. This made for very rapid development and demonstration of the device.

However, the original reconstruction software had to be modified in the following ways. In the Fourier plane, the new system produces six satellite images which are three pairs of data – each pair is associated with a single wavelength. For each pair, one of the data sets is windowed and extracted. Each data set is then multiplied by a wavelength dependent diffraction propagator. Other chromatic effects are also included in the propagator beyond just the wavelength dependent diffraction effects. For instance, also included is a wavelength dependent focus term that is due to: 1) the chromatic focal shift of the aspheric objective lenses and 2) slight longitudinal positioning errors between the aspheric

lenses. After the target was numerically focused at each unique wavelength, the three images also needed to be rescaled with respect to one another. Once each unique wavelength was properly focused and scaled, they were overlapped to produce the multi-wavelength image.

## 3. EXPERIMENTAL DATA

The multi-wavelength DHM was used to measure Euglena, which is a single-celled organism roughly 25 μm in length. The raw hologram and the reconstructed image is shown below in Figure 5.

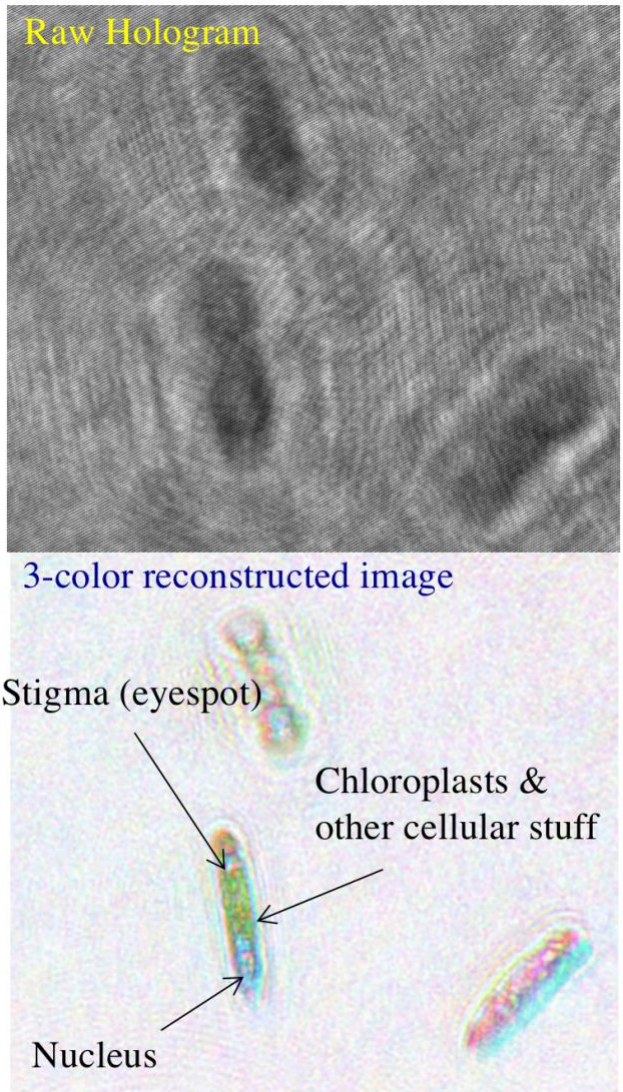


**Figure 5. The pseudo-color image of the bacteria Euglena was made with the multi-wavelength DHM. The three wavelengths used are: 405 nm, 488 nm, and 532 nm. This image is a still shot for a sequence taken at video rates (~15 frames per second).**

The three wavelengths used for this measurement where 405 nm, 532 nm, and 670 nm. The resolution of the image is about 0.7 μm, which is sufficient resolution to allow detection of sub-cellular structures such as the stigma (eyespot), nucleus, chloroplast, and other sub-cellular stuff. These measurements were made a video rates (roughly 15 frames per second), and reconstructed over about 10 seconds. During this time, the bacteria swam all over the field of view (360 μm x 360 μm) of the instrument. This motion of the species enabled methods for noise reduction in the following ways: 1) static optical aberrations can be removed by averaging over the full time series and subtracting, 2) the speckle noise which evolves over very short time scales can be averaged over only a few frames. Both methods were used to reduce the data and produce a color image with excellent color uniformity and superior spatial resolution.

Finally, we note that the instrument allows us to measure the phase of the object for the three different wavelengths. With proper calibration, this allows us to also get an estimate on the index of refraction of the sample being measured. This additional information can be used as a discriminator for biologic and mineral species.

## 4. SUMMARY

We have developed a new architecture for multi-wavelength digital holographic microscopy. This new instrument is strongly leveraged off of the original common-mode instrument, and shares the same benefits of that design: simplicity, robustness, stability, and sensitivity. We have used this instrument to measure biological samples and have recreated pseudo-color images at high resolution enabling us to discriminate and identify key morphologies within the cell. We will continue to develop this instrument for use in the lab and the field with the goal of refining the engineering for a future instrument for a lander targeted for the icy moons of the giant planets in our own solar system to search for microbial life.

## ACKNOWLEDGEMENTS

This work was carried out at the Jet Propulsion Laboratory, California Institute of Technology, under contract with the National Aeronautics and Space Administration.

Copyright 2018. All rights reserved.

## REFERENCES


[1] C. Knox, "Holographic microscopy as a technique for recording dynamic microscopic subjects," Science **153** (3739), 989-990 (1966).

[2] A. Chengala, M. Hondzo, and J. Sheng, "Microalga propels along vorticity direction in a shear flow," Phys. E. Stat. Nonlin. Soft Matter Phys. **87**(5), 052704 (2013).

[3] J. Sheng, E. Malkiel, J. Katz, J. Adolf, R. Belas, and A.R. Place, "Digital holographic microscopy reveals prey-induced changes in swimming behavior of predatory dinoflagellates," Proc. Natl. Acad. Sci. USA **104**(44), 17512-17517 (2007).

[4] J. Sheng, E. Malkiel, J. Katz, J. E. Adolf, and A. R. Place, "A dinoflagellate exploits toxins to immobilize prey prior to ingestion," Proc. Nath. Acad. Sci. UUSA **107**(5), 2081-2087 (2010).

[5] S. M. Vater, J. Finlay, M. E. Callow, J. A. Callow, T. Ederth, B. Liedberg, M. Grunze, and A. Rosenhahn, "Holographic microscopy provides new insights into the settlement of zoospores on the green alga *Ulva linza* on cationic oligopeptide surfaces," Biofouling **31**(2), 229-239 (2015)

[6] J. K. Wallace, S. Rider, E. Serabyn, J. Kühn, K. Liewer, J. Deming, G. Showalter, C. Lindensmith, and J. Nadeau, "Robust, compact implementation of an off-axix digital holographic microscope", Opt. Express 23, 17367-17378 (2015).

[7] J. Kühn, T. Colomb, F. Montfort, F. Charrière, Y. Emery, E. Cuche, P. Marquet, and C. Depeursinge, "Real-time dual-wavelenght digital holographic microscopy with a single hologram acquisition," Opt. Express 15, 7231-7242 (2007).

[8] J.L. Zhao, H.Z. Jiang, and J.L. Di, "Recording and reconstruction of a color holographic image by using digital lensless Fourier transform holography," Opt. Express 16, 2514-2519 (2008).

[9] B. Javidi, P. Ferraro, S.-H. Hong, S. De Nicola, A. Finizio, D. Alfieri, and G. Pierattini, "Three-dimensional image fusion by use of multiwavelength digital holography," Opt. Lett. 30, 144-146 (2005).

[10] U. Schnars and W. Juptner, "Digital recording and numerical reconstruction of holograms," Meas. Sci. Technol. 13(9), R85-R101 (2002).


## BIOGRAPHY

***J. Kent Wallace*** *received a B.S. in Physics/Mathematics from Rose-Hulman Institute of Technology in 1988, and an MS in Optics from the University of Rochester in 1992. He is an optical engineer at JPL with more then two decades of experience in optical instrumentation. His work includes optical stellar interferometry, nulling interferometry, adaptive optics, high-contrast imaging, and wavefront sensing and control. All of these activities have been focused on exoplanet detection. Recent research involves instrumentation for digital holographic microscopy as well as earth-observing instrumentation for greenhouse gas monitoring from space.*

***Gene Serabyn*** *is a Senior Research Scientist at JPL, having been with Caltech and JPL for thirty years. He works both on high-contrast coronagraphic and interferometric techniques for exoplanet detection, and on microscopic techniques for remote life detection.*

***Christian Lindensmith*** *received a B.S. in Physics from the University of Michigan in 1988. Before entering graduate school at the University of Minnesota in 1990 to earn a Ph.D. in Physics, he worked at a small superconducting wire company. After finishing graduate school in 1996, he went to the Jet Propulsion Laboratory where he has been active in developing missions, instruments, and technologies for detection of life away from Earth.*

***Jay Nadeau*** *got her PhD in theoretical nuclear physics from the University of Minnesota in 1996, then did an experimental postdoc in the laboratory of Henry Lester at Caltech until 2000. From 2000-2004 she was a scientist at the Jet Propulsion Laboratory, then assistant/associate professor of Biomedical Engineering at McGill University in Canada (2004-2015). She is currently an Associate Professor of Physics at Portland State University leading an interdisciplinary group that develops instruments and techniques for cellular imaging.*

***Stephanie Rider*** *is a Mechanical Engineer working in the Aeronautics Department at The California Institute of Technology. For the past decade, she has designed, fabricated, and assembled various mechanical systems including opto-mechanical instruments, wind tunnel models, medical devices, and robotic vehicles.*

***Manuel Bedrossian*** *received a B.S. in Mechanical Engineering from the University of California, Riverside in 2015. He has been involved with research at the California Institute of Technology since 2011, and in 2016 began graduate studies in the Andrew and Peggy Cherng Department of Medical Engineering, expecting to earn a Ph.D. in 2019. His research is focused on the development of robust imaging technologies that can be used to identify life in remote areas (e.g. icy moons). His research has applications in the medical field as these robust imaging techniques can be adapted to search for infectious diseases within the human body. Manuel hopes to devote his career towards expanding human knowledge about our own existence while at the same time developing medical devices to help better mankind.*